Vol. 8 (2015) *Acta Physica Polonica B Proceedings Supplement* No 4

PRODUCTION OF NEUTRONS IN THE VICINITY OF THE PION POLE*

B.Z. Kopeliovich, I.K. Potashnikova, I. Schmidt

Departamento de Física
and
Centro Científico-Tecnológico de Valparaíso
Universidad Técnica Federico Santa María
Casilla 110-V, Valparaíso, Chile

(Received November 12, 2015)

High-energy hadronic reactions with proton-to-neutron transitions (and *vice versa*) with small momentum transfer allow to study the properties of nearly on-shell pions, which cannot be accessed otherwise. We overview the recent results for such processes in deeply inelastic scattering, single- and double-leading-neutron production in pp collisions, including polarization effect. A special attention is paid to the absorption effects, which are found to be much stronger than what has been evaluated previously.

DOI:10.5506/APhysPolBSupp.8.977
PACS numbers: 13.85.Dz, 13.85.Lg, 13.85.Ni, 14.20.Dh

1. Preface

Nucleons are known to carry intensive pion clouds [1], which can be employed to study the pion properties. In particular, leading-neutron production was measured in deep-inelastic scattering (DIS) at HERA [2,3] aiming at extraction from data the pion structure function at small Bjorken x. In proton–proton collisions, leading-neutron production also offers an access to the pion–proton total cross section, which has been directly measured, so far with pion beams within a restricted energy range in fixed-target experiments. With modern high-energy colliders, the energy range for pion–nucleon collisions can be considerably extended. Measurements with polarized proton beams supply more detailed information about the interaction dynamics. Eventually, one can employ the unique opportunity to study pion–pion interactions in double-leading-neutron production in pp collisions. These processes, data and theoretical developments are briefly overviewed below.

* Presented by B.Z. Kopeliovich at EDS Blois 2015: The 16$^{\text{th}}$ Conference on Elastic and Diffractive Scattering, Borgo, Corsica, France, June 29–July 4, 2015.

2. Leading neutrons in DIS

Figure 1 (left) illustrates how the pion structure function can be measured in the reaction $\gamma^* p \to Xn$. The amplitude of this process in the Born approximation (no absorption corrections) has the form [4] of

$$A^B_{p\to n}(\vec{q}, z) = \bar{\xi}_n \left[\sigma_3\, q_{\rm L} + \frac{1}{\sqrt{z}}\, \vec{\sigma} \cdot \vec{q}_{\rm T}\right] \xi_p\, \phi^B(q_{\rm T}, z)\,, \tag{1}$$

where $\vec{\sigma}$ are Pauli matrices; $\xi_{p,n}$ are the proton or neutron spinors; $\vec{q}_{\rm T}$ is the transverse momentum transfer; $q_{\rm L} = (1-z)m_N/\sqrt{z}$; and z is the fractional light-cone momentum of the initial proton, carried by the final neutron.

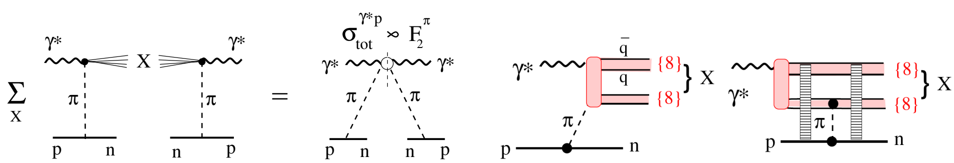

Fig. 1. Left: Graphical representation of the pion pole contribution to $\gamma^* p \to Xn$. Right: Absorption due to interaction of the debris from the $\gamma^*\pi$ inelastic collision.

At small $1-z \ll 1$, the pseudo-scalar amplitude $\phi^B(q_{\rm T}, z)$ has the triple-Regge form [5] of

$$\phi^B(q_{\rm T}, z) = \frac{\alpha'_\pi}{8}\, G_{\pi^+pn}(t)\, \eta_\pi(t)\, (1-z)^{-\alpha_\pi(t)} A_{\gamma^*\pi\to X}\left(M_X^2\right)\,, \tag{2}$$

where $M_X^2 = (1-z)s$; the 4-momentum transfer squared t has the form, $t = -q_{\rm L}^2 - q_{\rm T}^2/z$; and $\eta_\pi(t)$ is the phase (signature) factor which is nearly real in the vicinity of the pion pole. The effective vertex function $G_{\pi^+pn}(t) = g_{\pi^+pn}\exp(R_1^2 t)$, where $g^2_{\pi^+pn}(t)/8\pi = 13.85$. The value of the slope parameter R_1 is small [4, 5] and is dropped-off for clarity in what follows.

Correspondingly, the fractional differential cross section of inclusive neutron production in the Born approximation reads

$$\frac{1}{\sigma_{\rm inc}}\, \frac{d\sigma^B_{p\to n}}{dz\, dq_{\rm T}^2} = \left(\frac{\alpha'_\pi}{8}\right)^2 \frac{|t|}{z}\, g^2_{\pi^+pn}\, |\eta_\pi(t)|^2\, (1-z)^{1-2\alpha_\pi(t)}\, \frac{F_2^\pi\left(x_\pi, Q^2\right)}{F_2^p\left(x, Q^2\right)}\,, \tag{3}$$

where $x_\pi = x/(1-z)$; $\alpha'_\pi = 0.9$ GeV^{-2} is the pion Regge trajectory slope.

The Born approximation, Eqs. (2)–(3), is subject to strong absorption effects, related to initial and final state interactions of the debris of the $\gamma^*\pi$ inelastic collision, which can be presented as two color-octet $\bar{q}q$ pairs, as is illustrated in Fig. 1 (right). At high energies and large z, such a dipole should be treated as a 4-quark Fock component of the projectile photon, $\gamma^* \to \{\bar{q}q\}_8 - \{\bar{q}q\}_8$, which interacts with the target proton via π^+ exchange. This 4-quark state may also experience initial and final state interaction via vacuum quantum number (Pomeron) exchange with the nucleons (ladder-like strips in Fig. 1 (right)).

The absorption factor $S_{4q}(b)$ is naturally calculated in impact parameter representation, relying on the well-known parametrizations of the dipole cross section, measured at HERA. The amplitude and the absorption factor factorize in impact parameters, then, one should perform inverse Fourier transformation back to momentum representation. The details of this procedure can be found in [4].

The results of calculations are compared with data [2] for Q^2-dependence of the fractional cross section in Fig. 2 (left). The observed independence of Q^2 at large z is a direct consequence of the mechanism of absorption under consideration, shown in Fig. 1 (right). These results include, besides the pion exchange, also contributions from other iso-vector Reggeons, natural parity ρ and a_2, and unnatural parity $\tilde{a}_1$, which contains the weak a_1 pole and the strong ρ–π Regge cut [4, 6].

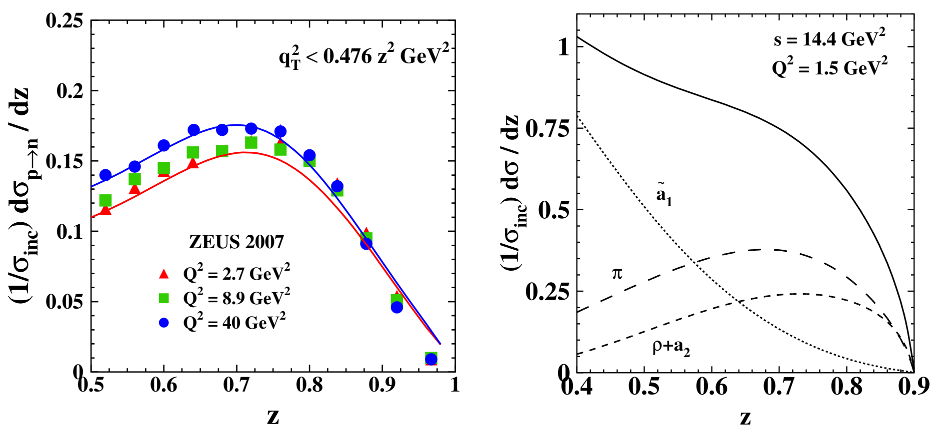

Fig. 2. Left: Comparison of the calculated Q^2-dependence of the fractional cross section of neutron production with data from [2]. Right: The tractional cross section calculated at $Q^2 = 1.5$ GeV^2 and $\nu = 8$ GeV.

Analogous measurements of leading proton production from a neutron target (deuteron) are planned to be done at the Jefferson Lab. An example of expected fractional cross section calculated at $Q^2 = 1.5$ GeV^2 and $\nu = 8$ GeV is presented in Fig. 2 (right). The relative contribution of the pion pole is smaller compared with low-x processes, therefore, the results are expected to be more model-dependent.

3. Single neutron production in *pp* collisions

Similar to DIS, production of leading neutrons at modern colliders (RHIC, LHC) offers a possibility to measure the pion–proton cross section at energies higher than have been available so far with pions beams. Otherwise, if the π–p cross section is known or guessed, one can predict the cross section of $pp \to pX$, which is given by the same expression as Eq. (3), except the last factor, the ratio F_2^π/F_2^p, should be replaced by $\sigma_{\rm tot}^{\pi p}(M_X^2)/\sigma_{\rm tot}^{pp}(s)$. The results of the Born approximation [7] are depicted by upper three curves in Fig. 3 (left), which agree with ISR data at $\sqrt{s} = 30.6$ and 62.7 GeV [8].

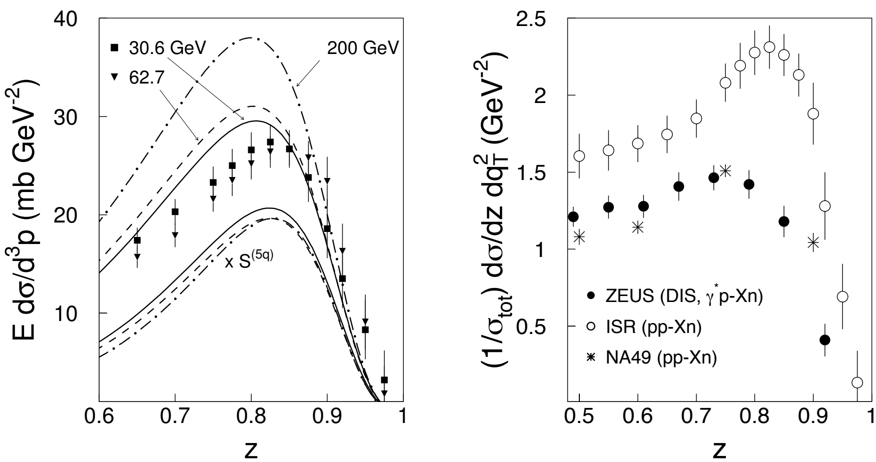

Fig. 3. Left: Energy dependence of the differential cross section of forward neutron production, calculated in the Born approximation (upper) and absorption corrected (bottom). Data are from [2]. Right: Comparison of fractional forward cross sections of neutron production in *pp* collisions [8, 11] and in DIS [2].

Of course, these Born approximation results should be corrected for the absorption effects, which were found in [9, 10] rather weak, in agreement with the ISR data. On the contrary, the absorption factor calculated in [7] leads to a much stronger suppression, close to what was found for DIS in the previous section. As a consequence, the absorption-corrected three bottom curves in Fig. 3 (left) strongly underestimate the data.

It was concluded in [7] that the normalization of the data [8] is incorrect. Indeed, the comparison with other currently available data in DIS [2] and in *pp* collisions [11] plotted in Fig. 3 (right) shows that, indeed, these fractional cross sections are about twice below the ISR data. One hardly can imagine that absorption in photon-production process is stronger than in *pp*.

The reason of weak absorption found in [9, 10] is explained in Fig. 4. The third Reggeon graph (c) was neglected because the 4-Reggeon vertex $2\mathbb{P}2\pi$ was claimed to be unknown. However, this vertex has a structure, shown in the right part of Fig. 4, and it gives the largest contribution to the absorption effects.

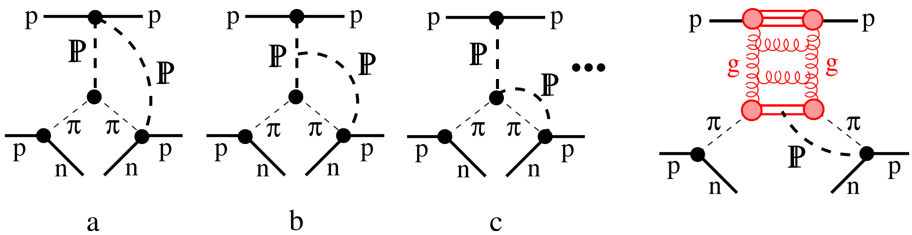

Fig. 4. Left: Triple-Regge graphs contributing to the absorption corrections. Right: The structure of the $2\mathbb{P}2\pi$ vertex in graph (c).

In addition to the cross section, the rich spin structure of the amplitude, Eq. (1), suggests a possibility of a stringent test of the dynamics of the process, supported by recent precise measurements of the single-spin asymmetry of neutron production at RHIC [12, 13]. Of course, the amplitude (1) does not produce any spin asymmetry because both terms have the same phase. However, the strong absorption corrections change the phase and spin effects appear. Nevertheless, the magnitude of $A_N(t)$ was found in [6] to be too small in comparison with the data.

Interference with natural parity Reggeons ρ and a_2 is strongly suppressed at high energies. Only the spin-non-flip axial-vector Reggeon a_1 is a promising candidate. Its effective contribution $\tilde{a}_1$ also includes the ρ–π Regge cut. The results of parameter-free evaluation of $A_N(t)$ [6] due to π–$\tilde{a}_1$ interference, shown by stars in Fig. 5 (left), agree well with data [12, 13].

4. Double-neutron production

The large experiments at the RHIC and LHC colliders are equipped with zero-degree calorimeters (ZDC), which can detect small angle leading neutrons. This suggests a unique opportunity to detect two leading forward–backward neutrons. According to Fig. 5 (right), one can extract from data precious information about pion–pion interactions at high energies.

The cross section of this process in the Born approximation has a factorized form [14] of

$$\frac{d\sigma^B(pp \to nXn)}{dz_1 dz_2\, dq_1^2 dq_2^2} = f^B_{\pi^+/p}(z_1, q_1)\, \sigma^{\pi^+\pi^+}_{\rm tot}(\tau s) f^B_{\pi^+/p}(z_2, q_2)\,, \tag{4}$$

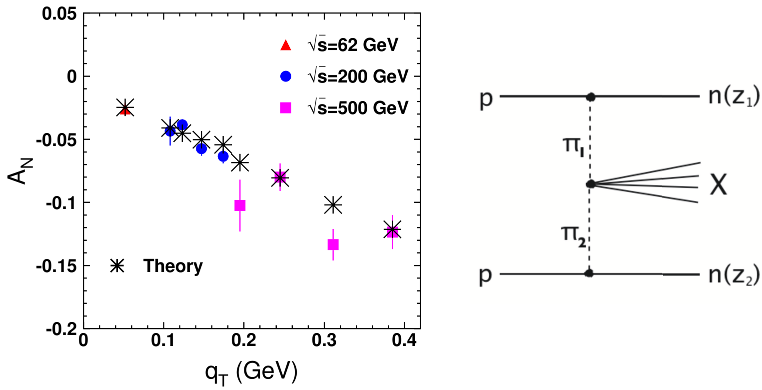

Fig. 5. Left: Comparison of the parameter-free calculations [6] (stars) with data [12]. Right: Double-pion exchange in the double-neutron production amplitude.

where the pion flux in the proton with fractional momentum $1-z$ reads [5]

$$f^{B}_{\pi^+/p}(z,q) = -\frac{t}{z}\, G^2_{\pi^+pn}(t)\left|\frac{\alpha'_\pi \eta_\pi(t)}{8}\right|^2 (1-z)^{1-2\alpha_\pi(t)} \,. \tag{5}$$

This flux at $q=0$ is plotted by dashed curve in Fig. 6 (left). The absorption-corrected flux is plotted by solid curve, demonstrating a considerable reduction [14].

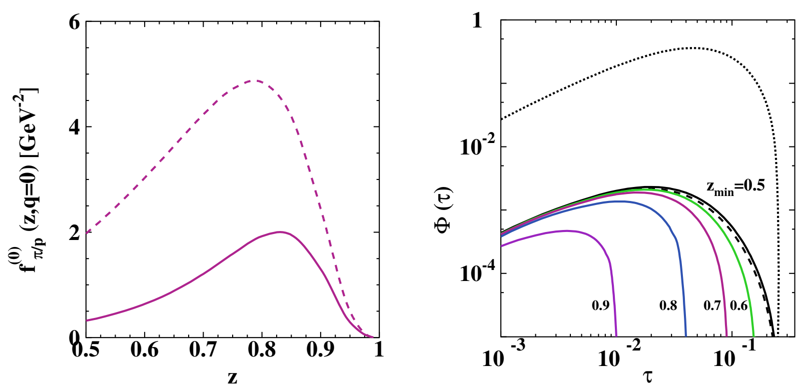

Fig. 6. Left: The forward flux of pions $f^{(0)}_{\pi^+/p}(z,q)$, calculated in the Born approximation (dashed) and including absorption (solid). Right: The integrated flux of two pions at $z_{\rm min}=0.5$ in the Born approximation (dotted), and absorption corrected (dashed). Solid curves with $z_{\rm min}=0.5$–0.9 also include the feed-down corrections.

To maximize statistics, one can make use of all detected neutrons, fixing $M_X^2 = \tau s = (1-z_1)(1-z_2)s$ to extract the $\pi\pi$ total cross section, $\sigma(pp \to nXn)_{z_{1,2}>z_{\min}} = \Phi^B(\tau)\,\sigma_{\rm tot}^{\pi^+\pi^+}(\tau s)$. The double-pion flux $\Phi(\tau)$ reads

$$\Phi(\tau) = \frac{d\sigma(pp \to nXn)_{z>z_{\min}}}{\sigma_{\rm tot}^{\pi^+\pi^+}(\tau s)} = \int \frac{dz_1}{1-z_1} F_{\pi^+/p}(z_1) F_{\pi^+/p}(z_2) D_{\rm abs}^{NN}(s,z_1,z_2)\,,$$

where $D_{\rm abs}^{NN}(s,z_1,z_2)$ is an extra absorption factor due to direct NN interactions, which breaks down the pion-flux factorization. This factor was calculated in [14]. The integrated pion flux $F_{\pi^+/p}(z)$ reads

$$F_{\pi^+/p}(z) = -z \int\limits_{q_{\rm L}^2}^{\infty} dt\, f_{\pi^+/p}(z,q)\,. \tag{6}$$

Thus, detecting pairs of forward–backward neutrons with the ZDCs installed in all large experiments at the RHIC and LHC, provides a unique opportunity to study the pion–pion interactions at high energies. However, the absorption effects are especially strong for this channel.

5. Summary

The higher Fock components of the proton, containing pions, allow to get unique information about the pion structure and interactions at high energies, provided that the kinematics of neutron production is in the vicinity of the pion pole. In this short overview, we presented several processes with neutron production, DIS on a proton, proton–proton collisions, including spin effects, and also double-neutron production. However, even in a close proximity of the pion pole, the analysis can hardly be performed in a model-independent way. Strong absorption effects significantly suppress the cross sections. We identified the main mechanism for these effects, which has been missed in previous calculations. It arises from the initial/final state interaction of the debris of the pion collision. It was evaluated employing the well-developed color-dipole phenomenology, based on DIS data from HERA.

B.Z.K. is thankful to the organizers of the EDS Blois Conference for the invitation to give a talk. This work was supported in part by Fondecyt (Chile) grants: 1130543, 1130549 and 1140390.

REFERENCES

[1] G.A. Miller, A.W. Thomas, S. Theberge, *Phys. Lett. B* **91**, 192 (1980).

[2] S. Chekanov *et al.* [ZEUS Collaboration], *Nucl. Phys. B* **776**, 1 (2007).

[3] F.D. Aaron *et al.* [H1 Collaboration], *Eur. Phys. J. C* **68**, 381 (2010).

[4] B.Z. Kopeliovich, I.K. Potashnikova, B. Povh, I. Schmidt, *Phys. Rev. D* **85**, 114025 (2012).

[5] B.Z. Kopeliovich, B. Povh, I.K. Potashnikova, *Z. Phys. C* **73**, 125 (1996).

[6] B.Z. Kopeliovich, I.K. Potashnikova, I. Schmidt, J. Soffer, *Phys. Rev. D* **84**, 114012 (2011).

[7] B.Z. Kopeliovich, I.K. Potashnikova, I. Schmidt, J. Soffer, *Phys. Rev. D* **78**, 014031 (2008).

[8] W. Flauger, F. Mönnig, *Nucl. Phys. B* **109**, 347 (1976).

[9] N. Nikolaev, W. Schäfer, A. Szczurek, J. Speth, *Phys. Rev. D* **60**, 014004 (1999).

[10] A.B. Kaidalov, V.A. Khoze, A.D. Martin, M.G. Ryskin, *Eur. Phys. J. C* **47**, 385 (2006).

[11] D. Varga [NA49 Collaboration], *Eur. Phys. J. C* **33**, S515 (2004).

[12] A. Adare *et al.* [PHENIX Collaboration], *Phys. Rev. D* **88**, 032006 (2013).

[13] Y. Goto [PHENIX Collaboration], *Phys. Part. Nucl.* **45**, 79 (2014).

[14] B.Z. Kopeliovich *et al.*, *Phys. Rev. D* **91**, 054030 (2015).